Macromolecular Bioscience

Solution behaviour of amphiphilic glycodendrimers with a rod-like core

--Manuscript Draft--

Manuscript Number:	mabi.201500452R1
Full Title:	Solution behaviour of amphiphilic glycodendrimers with a rod-like core
Article Type:	Full Paper
Section/Category:	
Keywords:	glycodendrimers; glycomimetics; morphological characterization; DC-SIGN; HIV
Corresponding Author:	Anna Bernardi Universita' di Milano Milano, ITALY
Corresponding Author Secondary Information:	
Corresponding Author's Institution:	Universita' di Milano
Corresponding Author's Secondary Institution:	
First Author:	Stefania Ordanini
First Author Secondary Information:	
Order of Authors:	Stefania Ordanini
	Giuliano Zanchetta
	Vanessa Porkolab
	Christine Ebel
	Franck Fieschi
	Ileana Guzzetti
	Donatella Potenza
	Alessandro Palmioli
	Črtomir Podlipnik
	Daniela Meroni
	Anna Bernardi
Order of Authors Secondary Information:	
Abstract:	Glycodendrimers based on aromatic cores have an amphiphilic character and have been reported to generate supramolecuar assemblies in water. We have recently described a new group of glycodendrimers with an aromatic rod-like core as potent antagonists of DC-SIGN mediated viral infections. A full characterization of the aggregation properties of these materials is presented here. The results show that these compounds exist mostly as monomers in water solution in dynamic equilibrium with small aggregates (dimers or trimers). Larger aggregates observed by DLS and TEM for some of the dendrimers were found to be portions of materials not fully solubilized and could be removed either by optimising the dissolution protocol or by centrifugation of the samples.
Additional Information:	
Question	**Response**
Please submit a plain text version of your cover letter here.	Dear Editor, please find attached that revised version of our manuscript Solution behaviour of amphiphilic glycodendrimers with a rod-like core modified according to the referees'

Please note, if you are submitting a revision of your manuscript, there is an opportunity for you to provide your responses to the reviewers later; please do not add them to the cover letter.	suggestions In particular, - at p. 27, we have corrected “sovramolecular” with “supramolecular” -we have revised the introduction (p. 4, new text highlighted in yellow) to blend-in the references to self-assembling systems and Janus glycodendrimers in a smoother fashion (we hope) We think this covers all the referees requests and look forward to your favorable decision. Best regards

DOI: 10.1002/marc.((insert number)) ((or ppap., mabi., macp., mame., mren., mats.))

Full Paper

Solution behaviour of amphiphilic glycodendrimers with a rod-like core[a]

Stefania Ordanini, Giuliano Zanchetta, Vanessa Porkolab, Christine Ebel, Franck Fieschi, Ileana Guzzetti, Donatella Potenza, Alessandro Palmioli, Črtomir Podlipnik, Daniela Meroni, Anna Bernardi*

Dr. Stefania Ordanini, Dr. Ileana Guzzetti, Dr. Donatella Potenza, Dr. Alessandro Palmioli, Dr. Daniela Meroni, Prof. Anna Bernardi
Università degli Studi di Milano, Dipartimento di Chimica, via Golgi 19, 20133 Milano, Italy
Dr. Giuliano Zanchetta
Università degli Studi di Milano, Dipartimento di Biotecnologie Mediche e Medicina Traslazionale, Via Fratelli Cervi 93, 20090 Segrate (MI), Italy
Vanessa Porkolab, Prof. Christine Ebel, Prof. Franck Fieschi
Univ. Grenoble Alpes, IBS, F-38044 Grenoble, France
CNRS, IBS, F-38044 Grenoble, France
CEA, IBS, F-38044 Grenoble, France
Prof. Črtomir Podlipnik
University of Ljubljana, Faculty of Chemistry and Chemical Technology, Večna pot 113, 1000 Ljubljana, Slovenia
Prof. Anna Bernardi
Università degli Studi di Milano, Dipartimento di Chimica, via Golgi 19, 20133 Milano, Italy
CNR-ISTM, Institute of Molecular Science and Technologies, Milano, Italy
E-mail: anna.bernardi@unimi.it, +39 0250314092

Glycodendrimers based on aromatic cores have an amphiphilic character and have been reported to generate supramolecuar assemblies in water. We have recently described a new group of glycodendrimers with an aromatic rod-like core as potent antagonists of DC-SIGN mediated viral infections. A full characterization of the aggregation properties of these materials is presented here. The results show that these compounds exist mostly as monomers in water solution in dynamic equilibrium with small aggregates (dimers or trimers). Larger aggregates observed by DLS and TEM for some of the dendrimers were found to be portions

[a] **Supporting Information** ((bold)) is available online from the Wiley Online Library or from the author.

of materials not fully solubilized and could be removed either by optimising the dissolution protocol or by centrifugation of the samples.

FIGURE FOR ABSTRACT

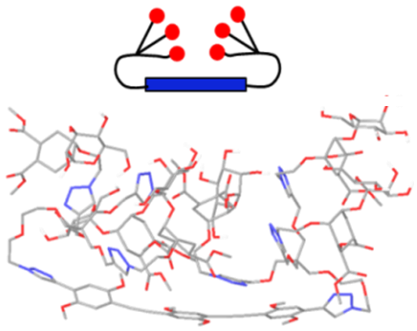

1. Introduction

Carbohydrate-protein interactions define a number of biological events, particularly in the early stages of cell adhesion to other cells, bacteria or viruses. Individual interactions between proteins and sugars are typically weak, but reach high avidity in living systems owing to multivalency on both the glycan and the protein side. This effect, often referred to as "the glycan cluster effect" or "the velcro effect", largely depends on the specific features of sugar binding proteins, called lectins, which tend to have large binding sites, rather flat and exposed to the solvent. To generate lectin antagonists able to outperform glycan clusters, researchers have relied on multivalent structures incorporating several copies of natural or unnatural ligands of moderate affinity on a polyvalent scaffold.[1-4] In particular, glycodendrimers have found widespread applications because they can be synthesized in a controlled fashion, allow full characterization of the final constructs and combine moderate valency with significant increase of relative inhibitory potency (RIP) per active unit involved.[5-8]

We[9] and others[10,11] have reported on glycodendrimers containing a rod-like aromatic core of variable length, which allows to span the large distances that separate lectins' binding sites. A previous study by our group[9] described the synthesis of a series of pseudo-glycosylated dendrimers (**Table 1**) assembled by linking a rod core and two trivalent dendrons. The dendrons carry glycomimetic compounds (either **4** or **6**, **Scheme 1**), designed to selectively antagonize DC-SIGN, a C-type lectin of the immune system. Depending on the length of the rod spacer, these constructs were found to achieve very high affinity for the target lectin and excellent control of DC-SIGN mediated HIV infection processes (IC_{50} in the nM range). Due to their modular structure and to the facile synthesis, constructs of this type can be easily tuned to match the geometrical properties of other relevant lectins and may have additional potential as an interesting novel class of glycodendrons.

The dendrimers shown in **Table 1** are characterized by an amphiphilic structure (**Scheme 1A**) and a limited solubility in water (up to 2-5 mM, **Table SI-1**), that may lead to the formation of aggregates in aqueous solution. A full characterization of their assembly behaviour in water is therefore essential to interpreting their lectin interaction properties and assessing the origin of their biological activity. Indeed, a number of amphiphilic glycodendrimers that self-assemble in water forming supramolecular aggregates of various size and shape have been reported.[12-16] Among them, so-called Janus dendrimers have been shown to generate complex supramolecular systems (nanoarchitectures) that are under active current investigation.[14] Controlled assembly of glycodendrimers can represent a desirable feature, as it allows to increase the system valency and size exploiting non-covalent interaction and generating systems with diverse topology, composition and assembly dynamics.[12,13]

To fully characterize the rod-based dendrimers of **Scheme 1**, the effect on the morphology in aqueous solution of the compound valence (either 2 or 6), rod length (either 1 or 3 repeating units) and active ligand moiety (either **4** or **6**) was evaluated. The structures and acronyms of the studied compounds are reported in **Table 1**. Due to the complexity of the structures and the potential confusions that can be generated in the literature, the numbering scheme of the original publication was maintained in this paper. Each dendrimer is numbered with a 3 digit acronym **x.y.z** where **x** represents the rod length (either 1 or 3 repeating units), **y** is a number indicative of the compound valence (**7** for a bivalent and **5** for a hexavalent compound) and **z** represents the glycomimetic moiety (either **4** or **6** for the ligands shown in **Scheme 1**). Typically, derivatives based on **4,** which features two aromatic amide moieties, have a lower water solubility than the corresponding structures bearing ligand **6**. The pseudo-sugar **4** was identified in previous studies as a DC-SIGN antagonist more potent and more selective than its parent ligand **6**.[17] The hexavalent dendrimer **3.5.4** is the most active species and blocks DC-SIGN mediated HIV infection in nanomolar concentration.[9] The analogue **3.5.6,** loaded with 6 copies of the pseudo-disaccharide **6**, is its closest, well-soluble model, and was used to

this end in this study. For every N-valent compound, only one sugar is depicted in **Table 1**: the other ones are replaced with a sphere for a matter of simplicity. Red spheres represent ligand **4**, blue spheres represent ligand **6**. Along the following paragraphs, the reader should refer to this scheme for molecular structures.

2. Results and Discussion

A preliminary assessment of the solution behaviour of the glycodendrimers was obtained by studying the effect of their concentration on the solution surface tension γ (**Figure 1**). A representative set was examined in a range of concentration from 0.05 mM to 2-5 mM (solubility limit); in all cases, the surface tension was found to decrease by increasing sample concentration. All compounds showed a rapid decay of γ at low concentrations followed by a slighter decrease at higher concentrations, but no plateau was reached. This differs from the classical behaviour of surfactants that typically display a quasi plateau of γ after reaching the critical micelle concentration. Nevertheless, the decrease of surface tension reflects the behaviour of molecules positively adsorbed at the air-water interface, which is typical of molecules having two different functionalities. This observation supports the hypothesis that the dendrimers have two explicit hydrophobic and hydrophilic functionalities. The trend shown by surface tension is consistent with the water solubility of the dendrimers (the less soluble are the compounds, the lower is their surface tension, see **Table SI-1**) but it does not unequivocally indicate the presence of aggregates. On the contrary, it suggests that, increasing sample concentration, the amount of free monomer that adsorbs at the interface increases as well. However, the formation of aggregates that adsorb at the interface and participate in the γ decrease cannot be ruled out; micelle-like material cannot show this kind of behaviour, but more complex aggregates may display hydrophobic moieties on their surface.

Computational studies were performed to model the aggregation behaviour of the dendrimers in solution. To this end, dynamics simulations of a cluster of 18 copies of **3.5.6** in TIP3P water solution were performed. We have previously reported[9] that a model of **3.5.6** with a non-pegylated rod core preferentially adopts the folded conformation shown in **Figure 2A**, possibly stabilized by sugar-sugar interactions. Eighteen copies of this structure were regularly distributed in a cubic box of 90 Å length. TIP3P water was added, the system was relaxed (by simulated annealing) and a 100 ns dynamics simulation was performed. In depth analysis of the trajectories did not show the formation of stable higher order structures. However, the dendrimers appear to aggregate, shielding the aromatic core from the water solvent while exposing the carbohydrate moieties. A dimer of dendrimers illustrating this interaction is shown in **Figure 2B**.

A second set of calculations (100 ns) were performed on the fully pegylated **3.5.6**, to analyze the influence of the PEG chains on the clustering behaviour. Also this system evolved towards the formation of clustered aggregates of similar structure, with an average coordination number of 4 (**Figure SI-2**) that were less tightly packed than those formed by the model non-pegylated dendrimers. A snapshot obtained after 60 ns of each simulation is shown in **Figure 2C,D** and is representative of the packing observed. The central dendrimer (green balls) is the one displaying the highest coordination number at this point of the simulation. Thus, the calculations show assembling behaviour of **3.5.6**, possibly driven by hydrophobic interaction of the aromatic cores, but do not suggest the formation of stable aggregates, at least on this timescale.

Dynamic Light Scattering (DLS), TEM and cryoTEM microscopies, Analytical Ultracentrifugation (AUC) and DOSY-NMR spectroscopy allowed us to investigate in more detail the solution behaviour of this class of glycodendrimers. Details of all these studies are reported as Supplementary Information. The results obtained for **3.5.4** and its more soluble model **3.5.6** are discussed below.

Preliminary DLS assays of **3.5.4** (0.15 mM in pH 8 water buffer, **Figure SI-3**) showed the presence of a monomeric species (1.3 nm radius, approximately 95 % of the mass distribution) and of large aggregates (500 nm radius) that clearly appeared to represent only a small percentage (about 5 %) of the molecules in solution. These aggregates were further characterized by DLS analysis at different concentrations, up to the solubility limit in water for both **3.5.4** and **3.5.6** (**Figure 3**). At all concentrations tested, **3.5.6** displayed a single (stretched) exponential decay of the correlation function, indicating a monomodal particle size distribution. The average hydrodynamic radius of the particles (R_H 50 nm) did not remarkably change varying the concentration from 0.06 to 0.6 mM, but approaching the solubility limit (data at 1.0 mM) larger assemblies (R_H = 150 nm) were observed, probably corresponding to incipient precipitating materials.

Large aggregates (R_H = 200 nm) were also observed for **3.5.4** at 0.12 mM, which represent the solubility limit of this compound in water solution. The morphological behaviour of **3.5.6** at 0.62 mM was tested also at 40 °C (not shown), revealing that temperature does not affect significantly the size of the aggregates. Testing **3.5.6** at the same concentration both in water and in buffer also gave comparable results (not shown). The width of Gaussian distribution reported in **Figure 3** (and in **Figure SI-4** for all other dendrimers) corresponds to the polydispersity estimated from the stretching exponent or from cumulant analysis of correlation functions. No evidence was found for depolarized scattering signal, which would be expected from anisotropic assemblies.

The polydispersity indication and the isotropic shape of the aggregates are consistent with images obtained by TEM and cryoTEM microscopy and shown in **Figure 4**. These images show the presence of nanometric spherical aggregates, characterized by a large polydispersity. Staining (phosphotungstic acid, **Figure 4A,B**) and cryo-imaging (**Figure 4D**) allow to appreciate the shape of the larger aggregates, which display less dense and softer cores. In principle, they could be vesicles or doughnut-like aggregates. The formation of doughnut-like

aggregates was reported by Prasad *et al.* for pyrene-modified polyamidoamine dendrimers in CH_2Cl_2 solution and attributed to hydrophobic interactions between pyrene units and hydrogen bonds between dendrimeric regions.[18] The aggregation of dendrimers in bilayer vesicles (called dendrimersomes) has been reported for non-symmetric dendrimers, called Janus dendrimers, constituted by linking two chemically distinct dendritic building blocks: a hydrophobic end and a hydrophilic one. Spherical, polygonal or tubular dendrimersomes have been reported upon injection of dendrimer solutions in water or buffer.[14] The formation of dendrimersomes has been reported also for amphiphilic Janus dendrimers bearing carbohydrates in their hydrophilic part.[13]

To achieve a clearer understanding of the nature of these aggregates and of their relation with the predominant monomeric species suggested by the DLS data, we resorted to Analytical Ultracentrifugation. Sedimentation Velocity Analytical Ultracentrifugation (SV-AUC) analyses were performed at 42000 rpm, at several concentrations of **1.5.4**, **1.5.6**, **3.5.4** and **3.5.6**, monitoring the absorption at several wavelength. All the tests performed are collected in **Table SI-3**.

The compounds were solubilised in the same buffer used for the DC-SIGN binding inhibition studies, which consists of 25 mM Tris-HCl (pH 8), 150 mM NaCl, 4 mM $CaCl_2$, 0.005 % P20 and includes 4 % of DMSO for **1.5.4** and **3.5.4**. It should be noted that P20 is a surfactant, used in the inhibition experiments to reduce non-specific interactions. In principle, the surfactant could also modify the aggregation properties of the glycodendrimers, therefore, to evaluate its role, the behaviour of selected compounds was investigated also in pure water, but no major differences were identified (see **Figure SI-7**).

For all compounds examined and independent on the solvent used (buffer or water) the sedimentation profiles show a largely prevalent species with sedimentation coefficients (*s*) very close to the value expected for the corresponding monomers (**Figure 5** and **Figure SI-7**). The sedimentation profiles observed for **3.5.6** between 0.01 and 1 mM are suggestive of a

possible dynamic equilibrium between a monomer (s_{theo},mono: 0.85 S) and a dimer (s_{theo},dimer: 1.2 S), which appears to shift towards the dimer as the concentration increases. However, the small difference between the predicted sedimentation coefficients of the two species could well fall within the experimental error. Small amounts of dimeric species (6 % - 11 %) were clearly identified in the sedimentation profiles of **3.5.4** at all tested concentrations in the range allowed by solubility limits (15 µM to 150 µM). Similar trends were observed for **1.5.6** and **1.5.4** (**Figure SI-7**). Thus, the SV-AUC data support the conclusion drawn from DLS experiments, but highlight that the predominant monomeric species are in dynamic equilibrium with small aggregates, possibly of the kind suggested by the computational model.

Interestingly, a loss of absorption was occasionally observed during the AUC experiments, as the centrifuge was speeded up to 42000 rpm (**Table SI-5**). This suggests that a small portion of the samples may exist as large aggregates that are pelleted at high rotational speed. Following this suggestion, DLS analysis of **3.5.6** 1.0 mM in water was performed before and after centrifugation of the sample. Different aliquots of the solutions were centrifuged for 1 h, 13 h or 40 h at 4000 rpm. Remarkably, already after 1 h, the intensity of the DLS signal associated with aggregates decreased by about 50 %. The mean size was also reduced, because of the faster sedimentation of the larger components in the distribution.

The intensity *I(t)* of the DLS signal associated with aggregates and the mean R_H of the sample kept decreasing by increasing the duration of the centrifugation, reaching a plateau after a few hours (**Figure SI-5**). It is noteworthy that when the 40 h-centrifuged sample was stocked for 4 weeks at 4 °C neither the intensity nor the hydrodynamic radius increased, indicating that, once removed, aggregates do not form anymore under these conditions.

The loss of signal upon centrifugation was investigated also through UV-Visible analyses. After centrifugation, the supernatant (65 µL) of the sample was separated through a syringe from the supposed pellet-containing solution (30 µL) and its absorbance was measured at 315

nm and 391 nm (**Table SI-2**), showing a decrease of up to 9 % compared to the original sample**.** These absorbance variations are consistent with those recorded through the spectrophotometer of the Analytical Ultracentrifugation machine (**Table SI-5**). Assuming that both the monomer and the aggregate have the same absorption coefficient, the observed absorbance variations indicate that the pelleted fraction of the samples corresponds to a small percentage (< 10 %) of the overall solution.

Overall, the results suggest that the large aggregates observed in the DLS experiments of **Figure 3** are composed by a fraction of molecules that have failed to dissolve rather than supramolecular assemblies. Indeed, when solubilisation of the samples was optimized by dissolving the dendrimers in DMSO at high concentration and diluting the solution with water or buffer to a final 4 % DMSO, aggregates were no longer detected by DLS for **3.5.6** (300 μM). A small amount of large aggregates was still visible for **3.5.4** (126 μM), but after centrifugation no absorbance loss was observed at 391 nm, suggesting that the pellet does not contain the rod chromophore.

Finally, DOSY-NMR spectra of **3.5.6** (D_2O, 298 K) showed no variation of diffusion coefficient (*D*, 0.88-0.96 × 10^{-10} m^2 s^{-1}) and corresponding hydrodynamic radius (R_H, 1.8-2.0 nm) in the available concentration range (1-4 mM, **Table SI-6**). The experimental value of R_H is comparable with the calculated dimension of the monomeric species (gyration radius 1.09 nm[9]), but the broad diffusion coefficient peak obtained (**Figure SI-8C**) seems indicative of the presence of several subpopulations in dynamic equilibrium.

3. Conclusions

A number of techniques were used to examine the aggregation behaviour of the rod-based glycodendrimers of **Table 1**. Whenever possible, analyses were performed both in water and

in Ca^{2+} containing buffer, representative of conditions that are employed for interaction studies of carbohydrates with C-type lectins, such as DC-SIGN. A range of different concentrations were explored, depending on the sensitivity of the techniques and on dendrimers' solubility.

Surface tension analysis (**Figure 1**) excluded the formation of micelles, as in classical surfactants, but supported the notion that the rod glycodendrimers possess two explicit hydrophilic and hydrophobic functionalities. Molecular dynamics simulations predicted that dendrimer **3.5.6** in water solution can generate loose assemblies of irregular size and shape (**Figure 2**). TEM and cryoTEM analyses of both **3.5.6** and **3.5.4** indeed showed highly polydispersed, nanometric aggregates (**Figure 4**). The larger ones are similar to doughnut-shaped materials or to perforated vesicles. Nonetheless, data from DLS, SV-AUC and DOSY-NMR clearly indicated that the prevailing species in solution is monomeric for all tested compounds.

The large aggregates (hundreds of nm) observed by DLS represent only a small percentage of the dendrimer mass in solution (**Figure SI-3**). Their full characterization by DLS, supported by AUC suggestions and UV-VIS analysis, allowed to establish them as a portion of molecules that have failed to dissolve and to optimize sample solubilisation. It was additionally shown that > 50 % of aggregates can be removed from concentrated samples by centrifugation and that aggregates represent only a small percentage (< 10 %) of the sample. Supernatant solutions removed after 40 h of centrifugation retain ≥ 90 % of the UV-Vis absorption intensity and do not show any new aggregate formation after 4 weeks at 4 °C.

SV-AUC analysis of the samples allowed detecting the formation of smaller assemblies, typically dimers, trimers and tetramers, albeit in very low amounts. The less soluble of the compounds analysed, **3.5.4** (solubility limit ≈ 150 μM), formed the highest amount of dimers (≈ 10 %, detected through AUC). The presence of several subpopulations in a dynamic

equilibrium centred on monomeric species was also supported by DOSY-NMR analysis of **3.5.6** in mM concentrations.

The results of this investigation firmly establish the physical context in which the biological activity of the examined glycodendrimers must be analysed. The potent DC-SIGN antagonism that characterise **3.5.4** in binding inhibition experiments and in infection studies[9] is not associated to the presence of supra-molecular, high valency assemblies, but rather is an intrinsic property of the monomeric species, which is certainly predominant at the nanomolar concentrations used in the biological tests, particularly when the samples are dissolved following the optimised procedure described here. Indeed, the previously reported infection studies were all performed starting from a 1mM stock solution of dendrimers in DMSO and diluting to the required concentration with the cell culture medium.

Rod-containing glycodendrimers hold a lot of promise for the development of tailored lectin-targeting devices, tuned to the specific size and shape of different receptors. The full characterization of their assembly properties in water solution reported in this paper will be instrumental for the development of these glycotools.

4. Experimental Section

The synthesis and characterisation of the glycodendrimers have been reported.[9]

4.1 Surface tension measurements.

Surface tension measurements of aqueous glycodendrimer solutions were performed with the pendant drop method using a Krüss EasyDrop instrument equipped with DSA1 software. The shape of the pendent drop was fitted using the Young-Laplace equation.

4.2 Molecular dynamics simulations.

Molecular dynamics simulations of pegylated and non-pegylated **3.5.6** were performed with YASARA Structure,[19] using the AMBER03 force field[20] under periodic-boundary conditions and with explicit TIP3P water. A multiple time step of 1.25 fs for intramolecular and 2.5 fs for intermolecular forces was used. In both cases, the initial configuration of the cluster consisted of 18 copies of dendritic molecules placed regularly into a cubic box with a length of 90 Å. The remaining available space in the box was filled with TIP3P water molecules. The final density of water objects in the cube was 0.997 g cm^{-3}. A 8.0 Å cutoff was used for Lennard-Jones forces. The Particle Mesh Ewald method was used to treat electrostatics.[21] At the start of the calculation, the system was minimized by simulated annealing, then dynamics simulations were run at 298 K. Temperature was adjusted using a Berendsen thermostat based on time-averaged temperature.[22] Dendrimers were parameterized with the AM1BCC protocol,[23] and atomic charges were assigned by applying simple additive bond charge corrections (BCCs) to AM1 atomic charges. All together 100 ns of molecular dynamics for each dendrimer (**3.5.6** pegylated and non-pegylated) were performed.

4.3 Dynamic Light Scattering (DLS).

Measurements were performed with a ST100 Scitech Instruments apparatus equipped with a laser (λ = 532 nm). Data were collected at a scattering angle of 90°, corresponding to scattering vector q ~ 0.022 nm^{-1}. Obtained correlation functions were fitted with Equation (1) using OriginPro8.5 software, to extrapolate the τ_c and α parameters.

$$G = y_0 + A^{-(\frac{\tau}{\tau_c})^{\alpha}} \quad (1)$$

The stretching exponent α gives an estimate of the polydispersity of the system (when α = 1, the single exponential decay is recovered, corresponding to a monodispersed system). The diffusion coefficient D of the scattering species was calculated from τ_c values and the corresponding R_H values were determined using the Stokes-Einstein equation. Compounds

were tested at different concentrations; water solutions of the compounds were filtered through a PTFE filter 0.45 μm, then lyophilized and re-solubilized in a filtered solvent (water or the SPR buffer, *i.e.* 25 mM Tris-HCl (pH 8), 150 mM NaCl, 4 mM $CaCl_2$. 4 % DMSO also included for dendrimers of ligand **4**). The preliminary data shown in **Figure SI-3** were obtained with a Dynapro Nanostar instrument.

4.4 Transmission electron microscopy (TEM)

Images were collected at room temperature using a Zeiss LEO 912ab Energy Filtering TEM operating at an acceleration voltage of 120 kV, equipped with a CCD-BM/1K system. Before dissolution, water solutions of the compounds were filtered through a PTFE filter 0.45 μm, then lyophilized and re-solubilized in filtered water. The sample preparation was carried out according to the following procedure. Aliquots of 5 μL of the compound solution were deposited onto Formvar-coated 300 mesh copper grids. The excess of water was then gently blotted using filter paper. When solvent evaporated at room temperature under atmospheric pressure, the grids were negatively stained by 1.5 wt % phosphotungstic acid. The aggregates diameters were measured by the EsiVision software (Olympus,Germany).

4.5 Cryogenic TEM (cryoTEM)

Images were recorded at -178 °C using a cryogenic sample holder GATAN915 in a Zeiss LIBRA 200FE-HR TEM, operating at 200 kV. Images were processed by means of the iTEM TEM Imaging Platform software (Olympus). The mean diameter and size distribution of the observed aggregates were obtained from a statistical analysis of over 270 aggregates. Before dissolution, water solutions of the compounds were filtered through a PTFE filter 0.45 μm, then lyophilized and re-solubilized in filtered water.

4.6 Sedimentation Velocity Analytical Ultracentrifugation (SV-AUC).

Analyses were performed in a Beckman XL-1 analytical ultracentrifuge using an AN-50 Ti rotor (Beckman instruments), at 20 °C. The experiments were carried out at 42000 rpm, using 50 µL, 100 µL or 430 µL samples in, respectively, two-channels 0.15 cm, 0.3 cm or 1.2 cm path length centrepieces equipped with sapphire windows (Nanolytics GmbH). The absorption was monitored at several wavelengths, depending on the absorption behaviour and concentration of solutions, with radial step size of 0.003 cm and time between profiles on a given sample of 20 min. In order to evaluate the role of the solvent, the compounds were solubilised either in water or in the same buffer solution used for SPR studies (*i.e.*, 25 mM Tris-HCl (pH 8), 150 mM NaCl, 4 mM $CaCl_2$, 0.005 % P20 ± 4 % DMSO). Several concentrations were tested, trying to approach also compounds' solubility limits. All performed tests are listed in **Table SI-3**. The distribution of sedimentation coefficients, *c(s),* were obtained from sedimentation velocity profiles, fitting several parameters (meniscus, bottom and frictional ratio f/f_{min}) with the SEDFIT software.[24] The partial specific volume ($\bar{v}$) of tested glycodendrimers was considered to be 0.7 $cm^3\ g^{-1}$, as a mean between values for hexose sugars and glycerol (about 0.6 and 0.77 $cm^3\ g^{-1}$).[25] Using SEDNTERP software, the viscosity and the density of the buffers were estimated to be 0.01023 poise and 1.005 g cm^{-3}, respectively. Water viscosity (0.01002 poise) and density (0.998 g cm^{-3}) are tabulated. For a regularization procedure, a confidence level of 0.68 was used.

4.7 Diffusion-Ordered NMR Spectroscopy (DOSY-NMR).

Experiments were performed on aqueous (D_2O) solutions of **1.7.6**, **3.7.6** and **3.5.6**. A range of concentrations (1-4 mM) was tested. NMR spectra were recorded on a Bruker AVANCE 400 MHz instrument, in D_2O at 298 K. Diffusion coefficients *D* were calculated with the module T1/T2 relaxation of the software Topspin, using the diffusion coefficient of D_2O (= $10^{-8}\ m^{-2}s^{-1}$) as internal standard. For each species and each concentration, reported *D* values are an

average of diffusion coefficients obtained for four different protonic regions. The hydrodynamic radii R_H were calculated using the Stokes-Einstein equation.

Supporting Information

Supporting Information is available from the Wiley Online Library or from the author

Acknowledgements: we thank Aline Le Roy (IBS) for technical assistance in the AUC experiments, Nadia Santo and Anna Ferretti (University of Milan) for assistance in the TEM and cryoTEM measurements. This work used the platforms of the Grenoble Instruct centre (ISBG; UMS 3518 CNRS-CEA-UJF-EMBL) with support from FRISBI (ANR-10-INSB-05-02) and GRAL (ANR-10-LABX-49-01) within the Grenoble Partnership for Structural Biology (PSB). Funding for Vanessa Porkolab's fellowship was provided by a grant from la Région Rhône-Alpes. In addition, this work was supported with funds from CM1102 COST Action.

Received: Month XX, XXXX; Revised: Month XX, XXXX; Published online:
((For PPP, use "Accepted: Month XX, XXXX" instead of "Published online")); DOI: 10.1002/marc.((insert number)) ((or ppap., mabi., macp., mame., mren., mats.))

Keywords: glycodendrimers, glycomimetics, morphological characterization, DC-SIGN, HIV

[1] A. Imberty, Y. M. Chabre and R. Roy, *Chem. – Eur. J.*, **2008**, *14*, 7490.

[2] A. Bernardi, J. Jiménez-Barbero, A. Casnati, C. De Castro, T. Darbre, F. Fieschi, J. Finne, H. Funken, K.-E. Jaeger, M. Lahmann, T. K. Lindhorst, M. Marradi, P. Messner, A. Molinaro, P. V. Murphy, C. Nativi, S. Oscarson, S. Penadés, F. Peri, R. J. Pieters, O.

Renaudet, J.-L. Reymond, B. Richichi, J. Rojo, F. Sansone, C. Schäffer, W. B. Turnbull, T. Velasco-Torrijos, S. Vidal, S. Vincent, T. Wennekes, H. Zuilhof and A. Imberty, *Chem. Soc. Rev.*, **2013**, *42*, 4709.

[3] N. P. Pera, R. J. Peters, *MedChemComm*, **2014**, *5*, 1027.

[4] S. Cecioni, A. Imberty, S. Vidal, *Chem. Rev.*, **2015**, *115*, 525.

[5] Y. M. Chabre, R. Roy, *Chem. Soc. Rev.*, **2013**, *42*, 4657.

[6] V. Wittmann, R. J. Pieters, *Chem. Soc. Rev.*, **2013**, *42*, 4492.

[7] Y. M. Chabre, R. Roy, *Adv. Carbohydr. Chem. Biochem.*, **2010**, *63*, 165.

[8] N. Rockendorf, T. K. Lindhorst, *Top. Curr. Chem.*, **2001**, *217*, 201.

[9] S. Ordanini, N. Varga, V. Porkolab, M. Thepaut, L. Belvisi, A. Bertaglia, A. Palmioli, A. Berzi, D. Trabattoni, M. Clerici, F. Fieschi, A. Bernardi, *Chem. Commun.*, **2015**, *51*, 3816.

[10] F. Pertici, N. Varga, A. van Duijn, M. Rey-Carrizo, A. Bernardi, R. J. Pieters, *Beilstein Journal of Organic Chemistry*, **2013**, *9*, 215.

[11] A. Barattucci, E. Deni, P. Bonaccorsi, M. G. Ceraolo, T. Papalia, A. Santoro, M. T. Sciortino, F. Puntoriero, *J. Org. Chem.*, **2014**, *79*, 5113.

[12] M. K. Müller, L. Brunsveld, *Angew. Chem. Int. Ed.*, **2009**, *48*, 2921.

[13] V. Percec, P. Leowanawat, H.-J. Sun, O. Kulikov, C. D. Nusbaum, T. M. Tran, A. Bertin, D. A. Wilson, M. Peterca, S. Zhang, N. P. Kamat, K. Vargo, D. Moock, E. D. Johnston, D. A. Hammer, D. J. Pochan, Y. Chen, Y. M. Chabre, T. C. Shiao, M. Bergeron-Brlek, S. André, R. Roy, H.-J. Gabius, P. A. Heiney, *J. Am. Chem. Soc.* **2013**, *135*, 9055.

[14] V. Percec, D. A. Wilson, P. Leowanawat, C. J. Wilson, A. D. Hughes, M. S. Kaucher, D. A. Hammer, D. H. Levine, A. J. Kim, F. S. Bates, K. P. Davis, T. P. Lodge, M. L. Klein, R. H. DeVane, E. Aqad, B. M. Rosen, A. O. Argintaru, M. J. Sienkowska, K. Rissanen, S. Nummelin, J. Ropponen, *Science*, **2010**, *328*, 1009.

[15] B. S. Kim, D. J. Hong, J. Bae, M. Lee, *J. Am. Chem. Soc.*, **2005**, *127*, 16333.

[16] L. Brunsveld, B. G. G. Lohmeijer, J. A. J. M. Vekemans, E. W. Meijer, *Chem. Commun.*, **2000**, *23*, 2305.

[17] N. Varga, I. Sutkeviciute, C. Guzzi, J. McGeagh, I. Petit-Haertlein, S. Gugliotta, J. Weiser, J. Angulo, F. Fieschi, A. Bernardi, *Chem. – Eur. J.*, **2013**, *19*, 4786.

[18] P. K. Lekha, E. Prasad, *Chem. – Eur. J.*, **2011**, *17*, 8609.

[19] E. Krieger, G. Vriend, *J. Comput. Chem.*, **2015**, *36*, 996.

[20] Y. Duan, C. Wu, S. Chowdhury, M. C. Lee, G. M. Xiong, W. Zhang, R. Yang, P. Cieplak, R. Luo, T. Lee, J. Caldwell, J. M. Wang, P. Kollman, *J. Comput. Chem.*, **2003**, *24*, 1999.

[21] U. Essmann, L. Perera, M. L. Berkowitz, T. Darden, H. Lee, L. G. Pedersen, *The Journal of Chemical Physics*, **1995**, *103*, 8577.

[22] H. J. C. Berendsen, J. P. M. Postma, W. F. van Gunsteren, A. DiNola, J. R. Haak, *The Journal of Chemical Physics*, **1984**, *81*, 3684.

[23] A. Jakalian, D. B. Jack, C. I. Bayly, *J. Comput. Chem.*, **2002**, *23*, 1623.

[24] a) P. Schuck, *Biophysical Journal*, **2000**, *78*, 1606;

b) www.analyticalultracentrifugation.com.

[25] H. Durchschlag, *Thermodynamic data for Biochemistry and Biotechnology*, Springer-Verlag Berlin Heidelberg, **1986**.

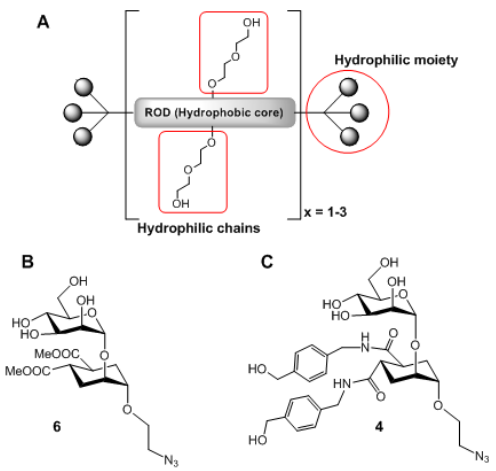

Scheme 1 (A) Schematic representation of rod derivatives, highlighting their modular structure and the amphiphilic components. (B) Structure of the pseudo-disaccharide **6**. (C) Structure of the pseudo-disaccharide **4**.

Table 1 Structures of tested compounds. Numbering and colour schemes as in the original communication.[9] Blue spheres represent ligand **6**, red spheres represent ligand **4**.

Structure	Cartoon	Numbering
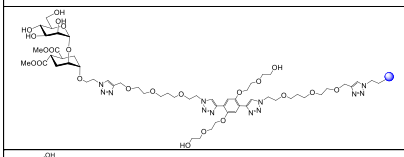		**1.7.6**
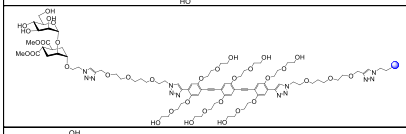		**3.7.6**
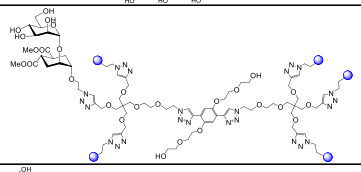	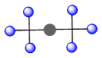	**1.5.6**
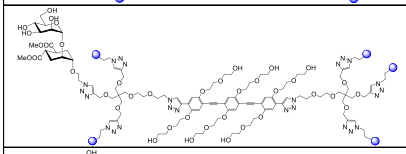		**3.5.6**
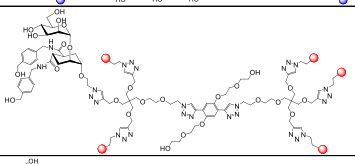	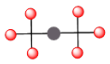	**1.5.4**
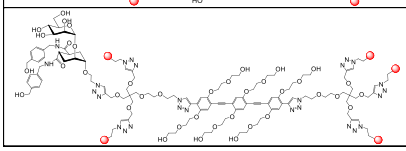		**3.5.4**

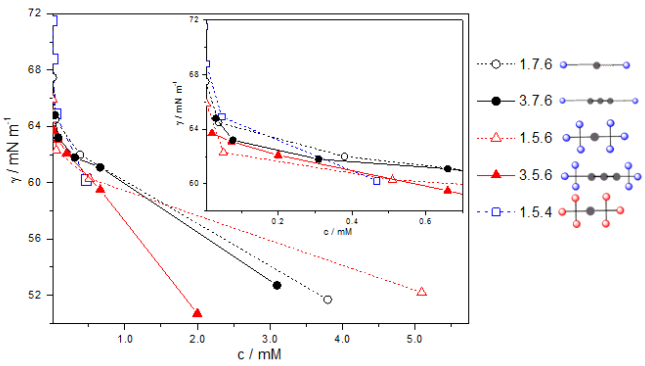

Figure 1 Surface tension of tested compounds in water as a function of concentration. Inset: Zoom in of low concentrations.

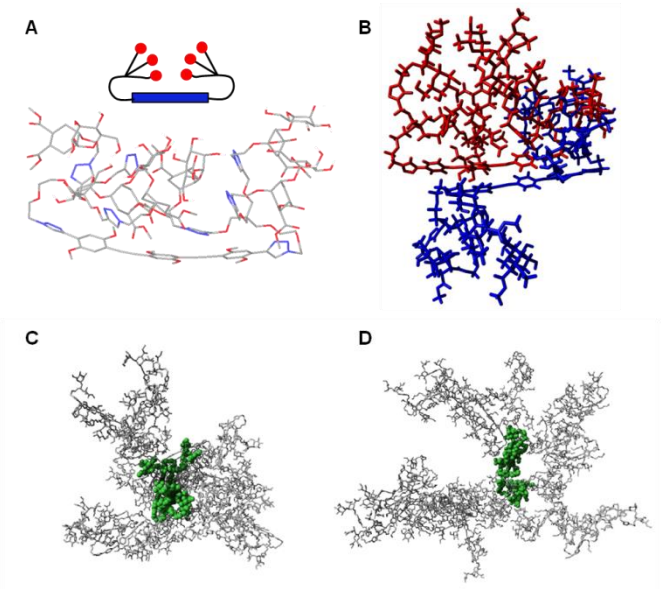

Figure 2 Dynamics simulations of dendrimer **3.5.6**. (A) Starting model of non-pegylated **3.5.6** (from ref.[9]). (B) Hydrophobic interactions between two rod cores appear to drive formation of dimers of dendrimers in a dynamic simulation (18 copies of **3.5.6** in TIP3P water). (C, D) molecular dynamics snapshot at 60 ns. Coordination around "central" dendrimer (dendrimer with highest coordination number at this point of the simulation). (C) non-pegylated dendrimer and (D) pegylated dendrimer.

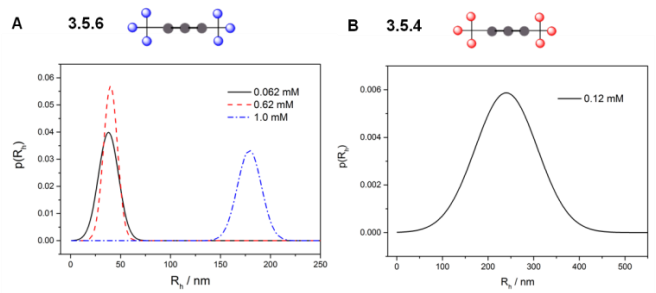

Figure 3 Size distributions extracted from DLS experiments for aqueous solutions of **3.5.6** (A) and **3.5.4** (B) at the concentrations indicated in the panels.

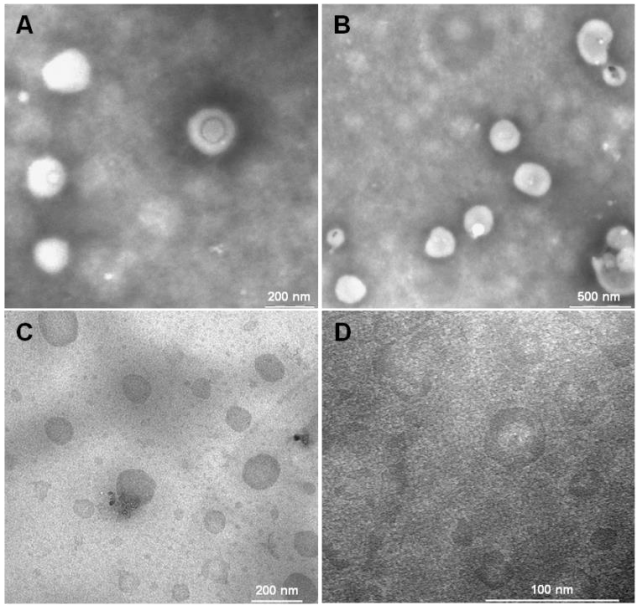

E

Mean	30 nm
Median	22 nm
Standard deviation	25 nm
Minimum	8 nm
Maximum	164 nm
Mode	15 nm

Figure 4 (A, B) TEM images of stained **3.5.6** 0.2 mM; (C) room temperature and (D) cryoTEM images of **3.5.4** 0.1 mM. Error bars are 200 nm (A), 500 nm (B), 200 nm (C) and 100 nm (D). (E) Diameter distributions calculated over 271 aggregates, from CryoTEM images of **3.5.4** 0.1 mM.

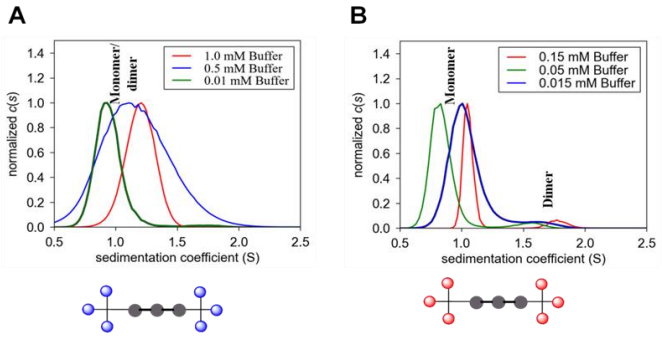

3.5.6		Conc. [mM]		
		1.0	**0.5**	**0.01**
Slow Boundary	s_{exp} (S)	1.2 (100 %)	1.2 (100 %)	0.94 (98 %)
	s_{theo},mono (S)	0.85	0.85	0.85
	s_{theo},dimer (S)	1.25	1.25	1.25
Fast Boundary	s_{exp} (S)	///	///	1.70 (2 %)
	s_{theo},trimer (S)	1.76	1.76	1.76

3.5.4		Conc. [mM]		
		0.15	**0.05**	**0.015**
Slow Boundary	s_{exp} (S)	1.05 (88 %)	1.02 (92 %)	0.83 (94%)
	s_{theo},mono (S)	1.00	1.00	1.00
Fast Boundary	s_{exp} (S)	1.78 (11 %)	1.78 (7 %)	1.51 (6 %)
	s_{theo},dimer (S)	1.59	1.59	1.59
	s_{theo},trimer (S)	2.08	2.08	2.08

Figure 5 c(s) distributions in sedimentation profiles of (A) **3.5.6** and (B) **3.5.4** solutions rotating at 42000 rpm at 298 K. In the tables, experimental sedimentation coefficients, s_{exp}, are compared to expected theoretical ones, s_{theo}, for globular particles, in buffer, with R_H corresponding to globular compact shape as reported in **Table SI-4**, and a partial specific volume fixed to 0.7 $cm^3\ g^{-1}$, as an average between values for hexose sugars and glycerol.

TOC

Amphiphilic glycodendrimers with an aromatic rod-like core that have been introduced as nanomolar inhibitors of DC-SIGN mediated HIV infection are now shown to be mainly monomeric in aqueous solution. Their efficiency as DC-SIGN antagonists, therefore, is proved to depend on their finely tuned morphology and not on self-assembled high-valent aggregates.

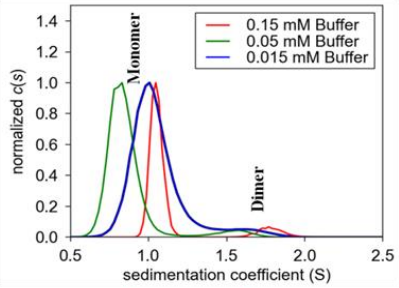

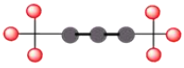

Click here to access/download

Production Data

Figures.zip